Proceedings of the
ASME Turbo Expo 2003
Atlanta, Georgia, June 2003

GT-2003-38634

BLADE EXCITATION BY AERODYNAMIC INSTABILITIES – A COMPRESSOR BLADE STUDY

Robert E. Kielb
Duke University

John W. Barter
GE Aircraft Engines

Jeffrey P. Thomas
Duke University

Kenneth C. Hall
Duke University

ABSTRACT

In this paper, we investigate non-synchronous vibrations (NSV) in turbomachinery, an aeromechanic phenomenon in which rotor blades are driven by a fluid dynamic instability. Unlike flutter, a self-excited vibration in which vibrating rotor blades and the resulting unsteady aerodynamic forces are mutually reinforcing, NSV is primarily a fluid dynamic instability that can cause large amplitude vibrations if the natural frequency of the instability is near the natural frequency of the rotor blade. In this paper, we present both experimental and computational data. Experimental data was obtained from a full size compressor rig where the instrumentation consisted of blade-mounted strain gages and case-mounted unsteady pressure transducers. The computational simulation used a three-dimensional Reynolds averaged Navier-Stokes (RANS) time accurate flow solver. The computational results suggest that the primary flow features of NSV are a coupled suction side vortex shedding and a tip flow instability. The simulation predicts a fluid dynamic instability frequency that is in reasonable agreement with the experimentally measured value.

INTRODUCTION

The two main aeroelastic phenomena considered in the design of turbomachinery blading are forced response and flutter. Forced response of rotor blades arises from aerodynamic excitations caused by circumferential variations in the flow field, such as those produced by upstream wakes. For a rotating blade, these excitations are steady in the reference frame of the stationery vane. As a result, the excitation frequencies occur at integer multiples of the vane passing frequency, and thus are said to be synchronous with the rotor speed.

Flutter, on the other hand, is a self-excited aeroelastic instability in which vibrating rotor blades and the resulting unsteady aerodynamic forces are mutually reinforcing. It is generally non-synchronous.

A third, less common form of aeroelastic vibration, non-synchronous vibration (NSV) has been seen in the front stages of high pressure compressor (HPC) and fan blades, vanes and blisks. This phenomenon, which is sometimes mistaken for flutter, has been seen by most, if not all, engine companies. In some instances, the unsteady loading has been to levels high enough to cause blade high cycle fatigue (HCF) failures. These failures require redesign of the component that is costly and can significantly increase engine development time.

Measured NSV vibrations are frequency and phase locked, and appear much like classical flutter. However, the values of typical flutter parameters (e.g. reduced frequency, incidence angle, Mach number) are well into the historically observed stable regions. In addition, the measured data implies that the response frequency is not necessarily the blade natural frequency (as is the case for classical turbomachinery flutter), and step changes in response frequency can be seen as the engine operating condition (speed and/or temperature) is varied. A possible explanation is that this phenomenon is driven primarily by an excitation source not dependent on blade vibrations.

In this paper, we present unsteady aerodynamic computational and experimental data for a first-stage compressor rotor blade where the excitation is believed to be due to a fluid dynamic instability, i.e., NSV.

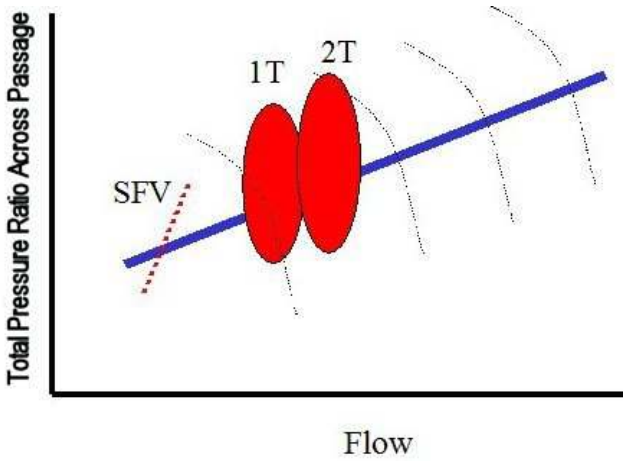

Fig. 1. Compressor map showing regions of NSV.

A representative example of NSV behavior is shown on the compressor map in Fig. 1. The shaded areas indicate regions where NSV response has been observed for front stage compressor rotors. The phenomenon usually occurs at part speed, but not necessarily on a high operating line. It can be affected by variable geometry, temperature, and operating conditions.

The case studied here is of a compressor rig test where the first stage compressor blades experience NSV. For this test, there are 35 rotor blades and 56 inlet guide vanes (IGV's). The radius ratio, blade aspect ratio, and tip solidity are approximately 1.6, 1.7, and 1.2, respectively. The tip clearance is 1.1% of the blade tip chord.

The stage 1 blades are observed to experience a significant first torsion mode (1T) response at lower speed that shifts to a second torsion mode (2T) response at somewhat higher speed. Figure 2 (further explained in the "Experimental Strain Gage Data" section) shows a typical plot of blade response frequency and amplitude versus rotational speed. The response at low speed is moderate separated flow vibration (SFV) response of the first flex (1F) and 1T modes. The SFV is a broad-band "buffeting" response of the blades. The blades are not frequency or phase locked, and usually vibrate in the first few blade modes to moderate response levels. This SFV 1F response is followed at higher speeds by a significant NSV, which excites the 1T mode to a high level of response. This response switches from a higher frequency (2661 Hz) excitation to a lower frequency (2600 Hz) excitation at a somewhat higher speed. As the speed increases, the response switches to a 2T mode excitation. Note that this low level 2T strain gage response is from a gage relatively insensitive to the 2T mode. The available data implies that the NSV response is not rotating stall.

The NSV problem has been addressed in a number of papers. One specific aspect that has received considerable attention is tip flow instability. Examples of work in this area can be found in Mailach (1999), Mailach et al. (2000 & 2001), Marz et al. (1999 & 2001), Inoue et al. (1999), Lenglin & Tan (2002), and Vo (2001). Mailach et al. (2001) present results from both a four stage low speed research compressor and a linear cascade, and conclude that the tip flow instability is a vortex interaction effect that produces a multi-cell circumferentially traveling wave. This phenomenon is found near the stall line with a relatively large tip clearance (greater than 2% of tip chord). A new Strouhal-type number is proposed to characterize the frequency of the oscillation. Marz et al. (2001) also found a tip flow instability on a low speed fan rig near the stall line and with a large tip clearance. This paper also presents the results of an unsteady CFD model that predicts a frequency of 950 Hz compared to the measured value of 880 Hz.

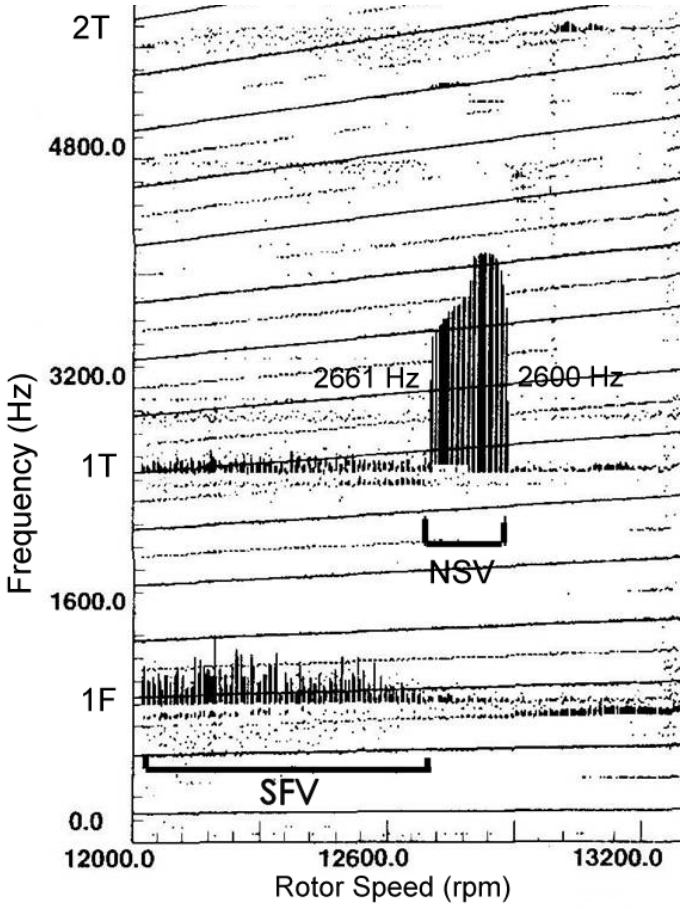

Fig. 2. Strain gage response of first-stage rotor blades of compressor rig.

Camp (1999) reports that this vexing problem has been observed in a high speed compressor. As a result, an experimental study was performed in a low speed compressor facility. A helical acoustic structure (circumferential Mach number of 0.84) was found using casing dynamic pressure transducers. It was also found that there were step changes in response frequency as the flow rate was changed. Although not

proven, the author speculates that the phenomenon involves vortex shedding from the blades that excites the helical acoustic cavity modes, which, in turn, excite the blades.

EXPERIMENTAL STRAIN GAGE DATA

As previously mentioned, the case studied herein is the NSV experienced by the first stage rotor blades of an instrumented compressor. There were 9 total strain gages mounted on the blades. All gages showed a frequency and phase locked NSV response in the 1T mode. An example was previously shown in Fig. 2. This data represents the blade response during slow rotor acceleration. The vertical lines at fixed values of rotor speed and frequency are a measure of blade response amplitude at that frequency. The NSV excitation of the 1T mode exists from approximately 12700 to 12880 rpm. As noted previously, there is a small decrease in NSV frequency at approximately 12800 rpm where the NSV frequency shifts from 2661 to 2600 Hz as the rotor speed increases.

EXPERIMENTAL CASING PRESSURE DATA

Unsteady pressure was also measured on the compressor casing at numerous axial and circumferential locations. Example data from a pressure transducer (located aft of the rotor 1 blades near the stage 1 vanes) is shown in Fig. 3. Significant response at frequencies of 3516 Hz and 3662 Hz was observed at all axial and circumferential measurement locations. Note that these response frequencies are measured in the non-rotating reference frame and are Doppler shifted from those seen in the rotating reference frame.

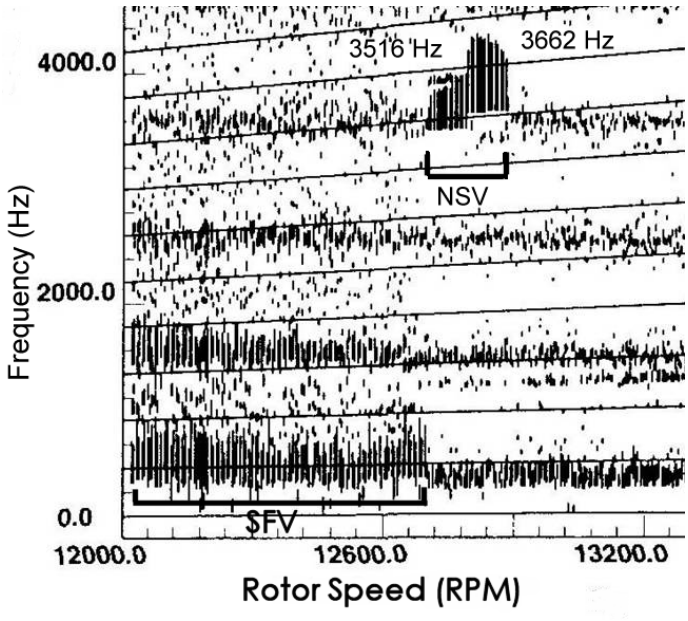

Fig. 3. Casing unsteady pressure measurements.

COMPUTATIONAL APPROACH

The unsteady CFD code, TURBO, (Chen & Briley (2001)), was used to investigate the NSV observed in the rig test. A single row, five passage, mesh modeled one-seventh of the rotor circumference. The mesh, consisting of 188 axial, 56 radial, and 280 circumferential grid points, contained approximately three million grid points. Passive coupling with the inlet guide vane was modeled by applying the steady solution downstream of the IGV's as an upstream boundary condition for the unsteady analysis of the rotor blades. In-phase boundary conditions on the circumferential edges of the computational domain were applied. This is consistent with the flow features caused by the IGV wakes, however, it restricts the allowable circumferential modes to multiples of seven nodal diameters (including zero). As discussed later, this restriction may change the circumferential wave speed and frequency. The simulation did not include blade motion, which eliminates classical flutter as a mechanism for unsteadiness. An example solution (entropy contours) at mid-span for one instant of time is shown in Fig. 4. As can be seen, the primary unsteadiness at this spanwise location is due to the IGV wakes.

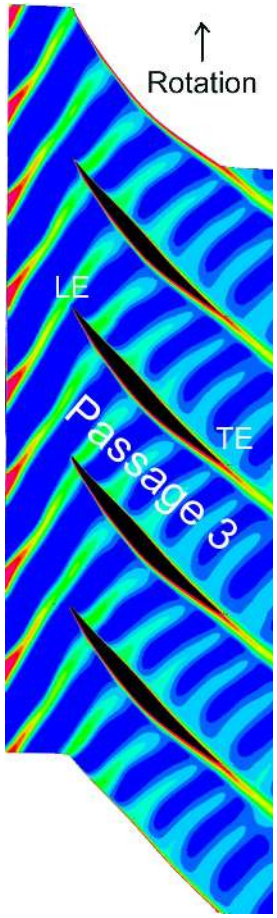

Fig. 4. Entropy contours at mid-span of rotor blades (five passages shown).

RESULTS – CIRCUMFERENTIALLY AVERAGED PROPERTIES

Fig. 5 shows the total inlet and outlet physical flow as a function of time (0.00042 seconds per iteration). There is an initial transient of approximately 0.006 seconds before the solution converges to a periodic oscillation. Fourier analysis of the periodic data indicates a dominant frequency of 2365 Hz. A plot of instantaneous absolute total pressure ratio versus instantaneous inlet corrected mass flow (both circumferentially averaged) is shown in Fig. 6. Note that the total variations in flow and pressure ratio are 1.3% and 0.8%, respectively. The oscillation of this instantaneous operating point is also found to have a dominant frequency of 2365 Hz with a significant harmonic content at 4730 Hz. The NSV phenomenon responsible for this response will be described subsequently. These results show that the NSV is not just a local blade excitation effect. That is, the global properties of the entire rotor row are oscillating.

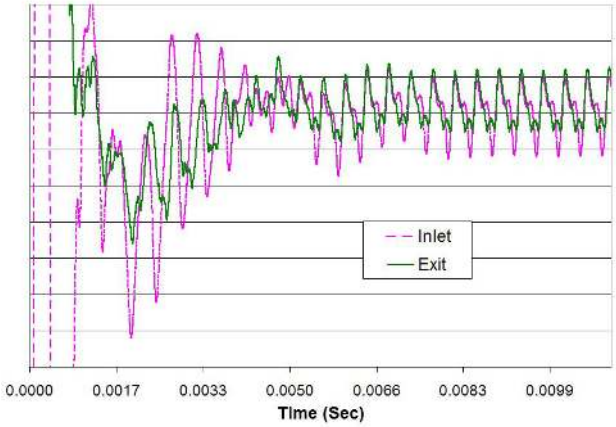

Fig. 5. Total physical flow.

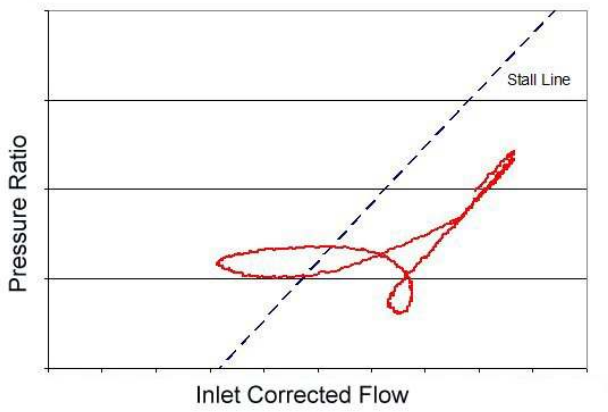

Fig. 6. Oscillation of pressure ratio and corrected flow.

RESULTS – BLADE SURFACE PRESSURES

The local unsteady static pressures from the periodic CFD solution were investigated at 70 locations on the blade surface. Fig. 7 shows the frequency domain results for a location in passage three, at mid-span near the leading edge on the suction side.

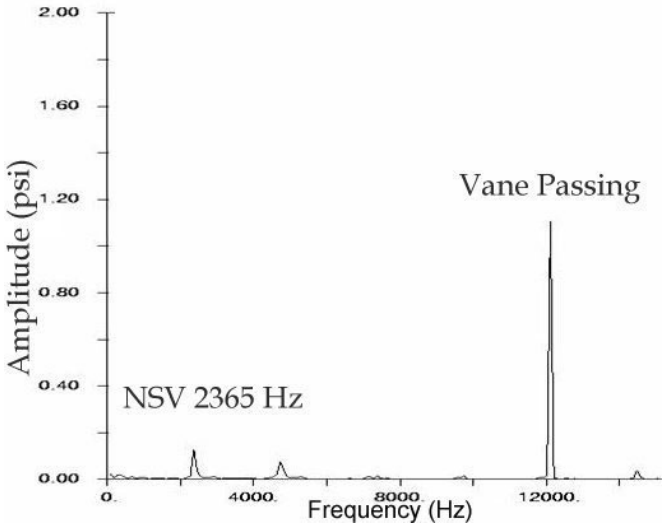

Fig. 7. Unsteady static pressure midspan suction side near the leading edge.

The response shows a predominance of vane passing frequency (12061 Hz). In addition there are minor peaks at 2365 Hz, and higher harmonics of this frequency. The character of the static pressure unsteadiness is significantly different near the blade tip. This is shown in Fig. 8, where the unsteady static pressures in passage three, near the leading edge on the pressure side, are presented.

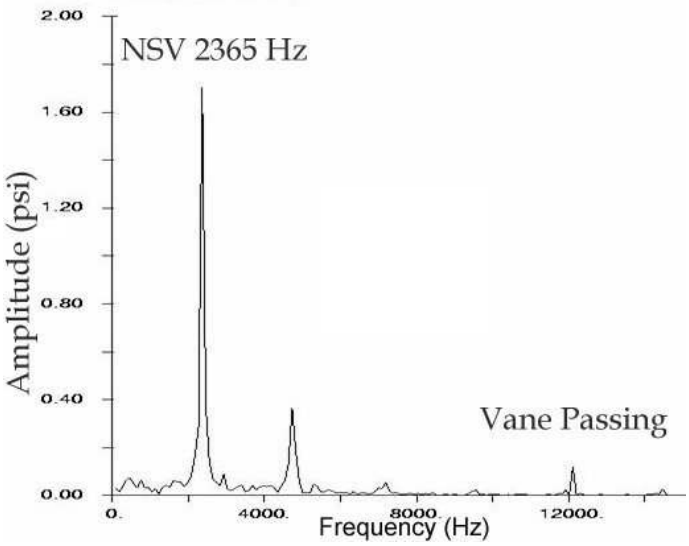

Fig. 8. Unsteady static pressure near tip pressure side near leading edge.

As can be seen, the unsteady pressure content at 2365 and 4370 Hz overwhelms that at the vane passing frequency. Although not shown, analysis of the unsteady static pressure data at identical locations in the other four passages indicates nearly the same amplitude and phase. Flow visualization of the computed unsteady solution also confirmed that all passages are experiencing nearly the same in-phase NSV phenomenon. Surprisingly, the phenomenon is in-phase for all blade passages. This represents an excitation source with 35 nodal diameters. (zero interblade phase angle, or 35 cells using rotating stall terminology). Note that this may be forced because of the boundary conditions on the circumferential edges of the computational domain.

The variation of the frequency content at four locations (pressure side mid-span, suction side mid-span, pressure side near the tip, and suction side near the tip) versus chordwise position is shown in Fig. 9 through Fig. 12, respectively. The mid-span location (Fig. 9 and Fig. 10) is dominated by vane passing excitation (12108 HZ). As expected, the vane passing excitation is highest near the leading edge and decays with distance down the chord. The NSV excitation is an order of magnitude lower in amplitude at this spanwise location.

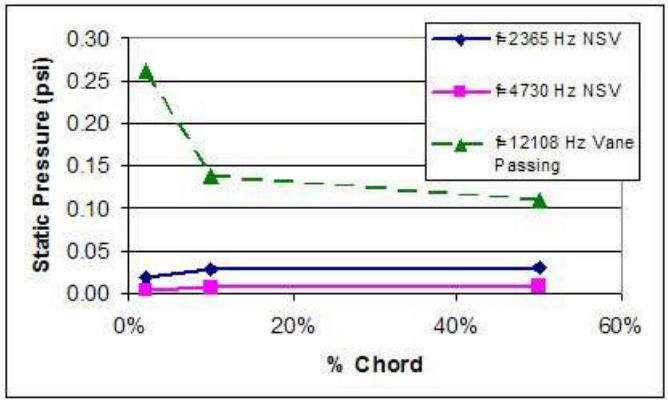

Fig. 9. Mid-span pressure side unsteady static pressures.

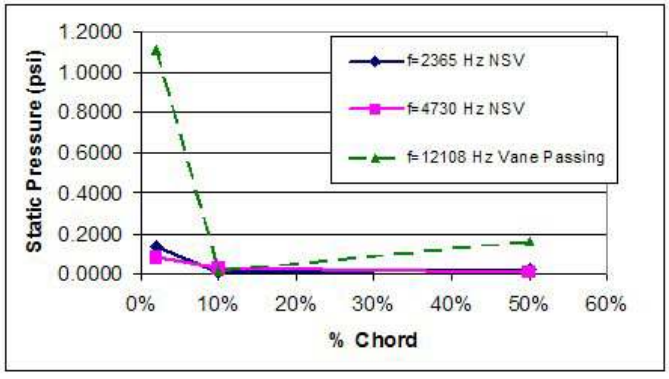

Fig. 10. Mid-span suction side unsteady static pressures.

In contrast, the unsteady pressure near the tip on the pressure side (Fig. 11) is dominated by NSV with the amplitude being an order of magnitude higher than that caused by vane passing. The predicted NSV frequency (2365 Hz) is approximately 9% lower than that measured in the rig test. The NSV excitation on the pressure side is highest near the leading edge and decays rapidly with distance down the chord. The suction side near the tip (Fig. 12) shows relatively low amplitude for both the NSV and vane passing excitations. In Figs. 11 and 12, the 120% chordwise location is aft of the airfoil on the same radial grid location as the points on the airfoil surface.

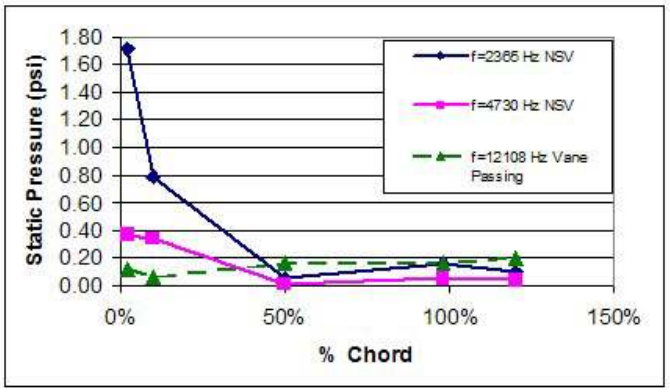

Fig. 11. Tip pressure side unsteady static pressures.

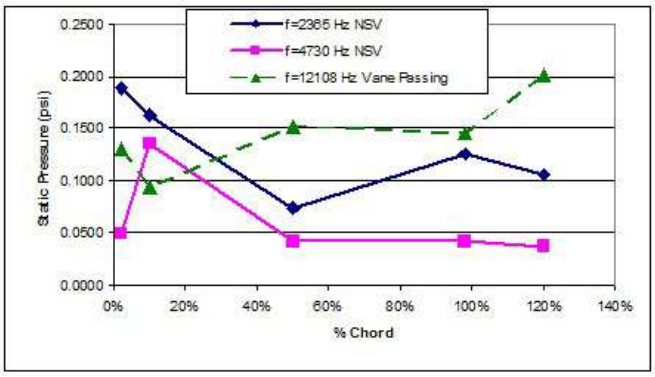

Fig. 12. Tip suction side unsteady static pressures.

RESULTS – CASING PRESSURES

An analysis of the computed casing unsteady pressures was conducted at approximately the same axial location as the measured data shown in Fig. 3. The resulting Fourier content is shown in Fig. 13. The dominate frequencies are related to blade passing with the unusual result that the 2X blade passing amplitude is approximately twice that of 1X. The NSV excitation appears at 5200 Hz and is somewhat lower in amplitude than 1X blade passing. For a 35 nodal diameter excitation source the frequencies of 2365 Hz (rotating reference frame) and 5200 Hz (non-rotating reference frame), correspond to an excitation source that rotates at 31% of rotor speed in the opposite direction of rotation. It is interesting that this is similar to the rotational speeds observed for stall cells. Note that this

predicted NSV frequency, as observed in the non-rotating reference frame is significantly different than that measured (3516 & 3662 Hz). This can possibly be explained by either an error in the circumferential speed and/or the number of nodal diameters of the NSV. Specifically, two ways that the experimental data can be explained are a 35 nodal diameter excitation rotating at 52% of rotational speed with respect to the rotor, or a 24 nodal diameter excitation rotating at 31% of rotor speed.

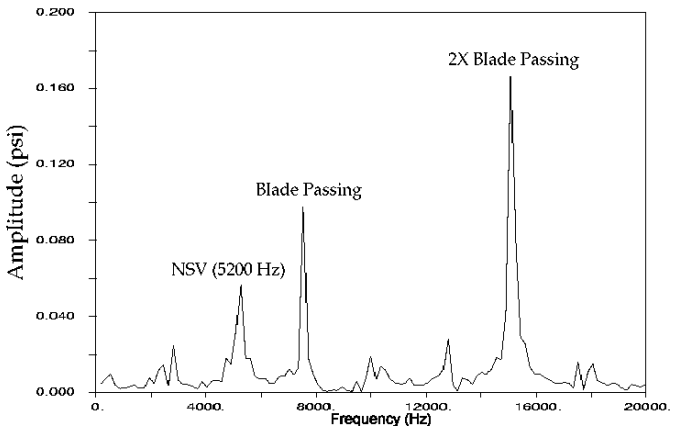

Fig. 13. Casing (non-rotating reference frame) frequencies.

UNSTEADY FLOW PHYSICS

It has been found that contour plots of entropy are valuable in tracking the features of this NSV excitation phenomenon, with animations being extremely useful. The NSV excitation had little effect at less than 70% span where the unsteadiness was dominated by vane passing excitation. This is consistent with the previously described blade surface unsteady static pressure data. and show entropy contours for passage three at four times (0, 90, 180, and 270 degrees of phase) during a period of NSV oscillation.

shows entropy contour plots at 98.1% span. In these figures the leading edge is on the left side, “SEI” denotes a small entropy island, and “LEI” denotes a large entropy island. At the “start” of the cycle three entropy islands can be seen: 1) a “finger” emanating near the leading edge at the top of the passage (suction side), 2), a large island near the middle of the passage, and 3) an island near 20% of chord at the bottom of the passage (pressure side). At one-quarter cycle the finger high entropy zone has split into a small island that is axially upstream of the blade leading edge, and a large entropy zone that is on the suction side near the leading edge. The island that was on the pressure side has now moved down the chord. At one-half cycle, the small entropy island is approaching the leading edge of the blade at the bottom of the passage, the suction side island is starting to move across the passage and the mid-passage island is approaching the pressure side of the blade at the bottom of the passage. At three-quarter cycle, the small island is starting to wrap around the leading edge of the airfoil at the bottom of the passage, and the mid-passage island has impacted the pressure side. The circumferential velocity of these islands is 31% of rotor speed opposite the direction of blade rotation, and is consistent with a fundamental frequency of 2365 Hz.

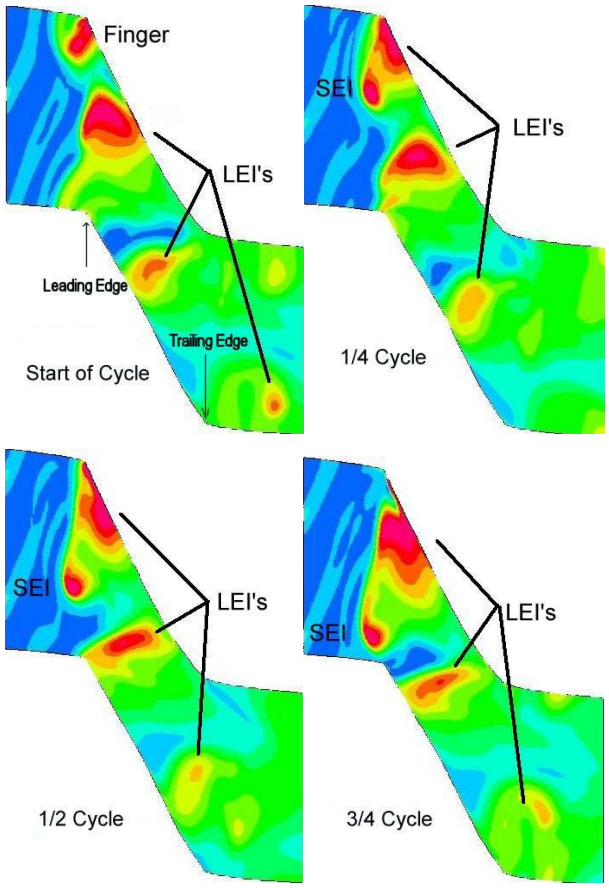

Fig. 14. Entropy contours near tip.

To examine the radial characteristics of this NSV phenomenon, entropy contours were examined on a plane of constant grid i value (a plane approximately normal to engine axial)). Contours at about 6% chord are shown in in a forward looking aft orientation.

At the start of the cycle an island of entropy can be seen at approximately 75% span just off of the suction side. This is a vortex that has been shed off the suction side leading edge. The region of high entropy near the case at mid-passage is the same mid-passage LEI seen in. At one-quarter cycle the suction side entropy has migrated radially outward, and the mid-passage LEI has moved toward the pressure side. At one-half cycle the suction side entropy has coalesced with the finger of entropy emanating from the tip clearance region. Analysis of the velocity vectors (not-shown) reveals that this zone corresponds to an oscillation in the angle of the clearance flow from the pressure to the suction side. The contour plot at one-half and

three-quarter cycle shows the of the vortex unsteadiness on the suction side at 75% span.

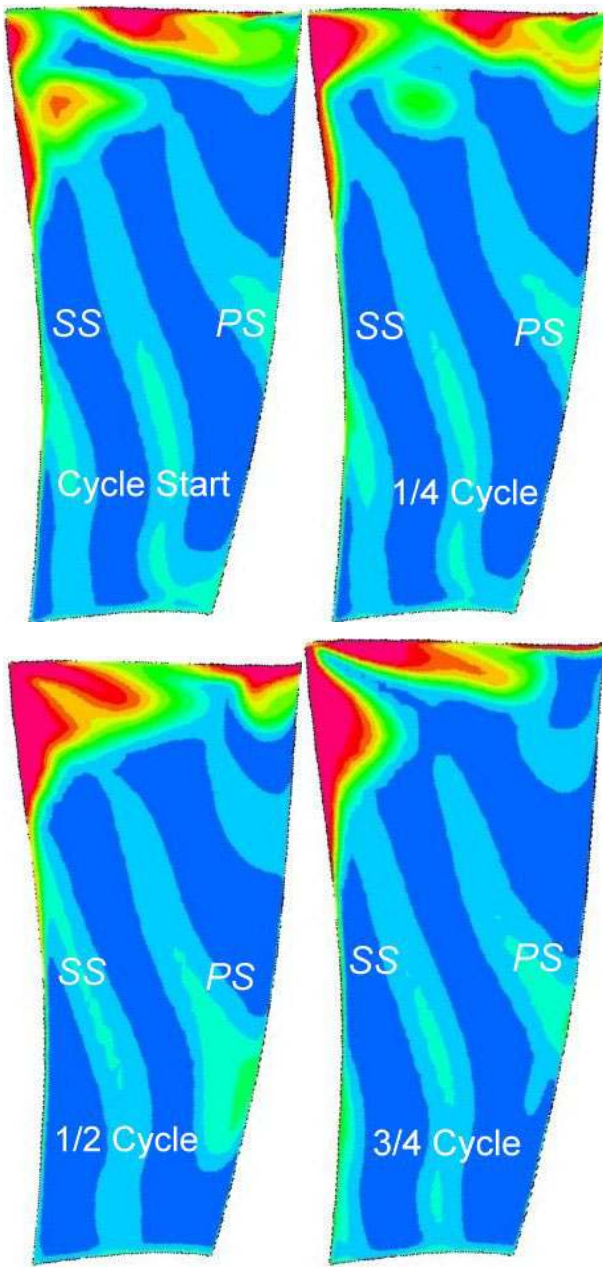

Fig. 15. Entropy contours near leading edge.

To summarize, the NSV instability unsteady flow physics primarily consists of two coupled unsteady aerodynamic features:

1) Separation/vortex unsteadiness on suction side near 75% span
   a) Occurs at zero to 20% of chord
   b) moves off airfoil surface and decays, but does not transport across passage
   c) high entropy zone moves radially out the span to interact with tip flow instability
2) Tip flow oscillation near leading edge
   a) primarily an oscillation in flow angle
   b) generates small entropy island (SEI) which traverses circumferentially slightly ahead of the blade leading edge
   c) when the SEI wraps around the leading edge of the adjacent blade the primary perturbation in tip flow occurs, and the process repeats itself
   d) rotates at 4082rpm (31% of rotor speed) relative to blades in opposite direction of rotation
   e) generates large entropy island which traverses passage, rides along pressure side, and produces large unsteady pressures near the leading edge that excite the 1T mode

SUMMARY AND CONCLUSIONS

Numerical simulations and experimental data for a non-synchronous excitation phenomenon have been presented for a first-stage compressor rotor. The numerical results show that the NSV is primarily a coupled suction side vortex unsteadiness (near 75% span) and tip flow instability. In the numerical simulation, the fluid motion in all passages is in phase, and the global properties, such as pressure ratio and flow, oscillate at the NSV frequency. The simulation predicts an aerodynamic instability frequency (blade reference frame) that is in reasonable agreement with the measured value. The frequency comparison in the non-rotating reference frame is poor, and may be due to the restrictions imposed by the boundary conditions on the circumferential edges of the computational domain. The maximum unsteady pressure due to the NSV is on the pressure side near the leading edge, and is significantly higher than the maximum unsteady pressure induced by IGV passing. Also at this location, the amplitude of the first harmonic of the NSV is significantly smaller, being near the same magnitude as that of the vane passing. A future paper will address the NSV characteristic frequency and compare the results of the case studied in this paper with the models proposed by previous researchers.

ACKNOWLEDGEMENT

The authors wish to acknowledge GE Aircraft Engines for financial support and for permission to publish this work.

REFERENCES

Camp, T. R., 1999, “A Study of Acoustic Resonance in a Low-Speed Multistage Compressor,” ASME Transactions Journal of Turbomachinery, Vol. 121, Number 1, Jan. 1999.

Chen, J.P., and Briley W.R., 2001, "A Parallel Flow Solver for Unsteady Multiple Blade Row Turbomachinery Simulations," ASME-2001-GT-0348, June 2001.

Inoue, M., Kuroumaru, M., Tanino, T., Furukawa, M., 1999, "Propagation of Multiple Short Length-Scale Stall Cells in an Axial Compressor Rotor," ASME Paper 99-GT-97.

Lenglin, G. and Tan, C. S., 2002, "Characterization of Wake- and Tip-Vortex Induced Unsteady Blade Response in Multistage Compressor Environment," 7th National Turbine Engine HCF Conference, May 2002.

Mailach, R., 1999, "Experimental Investigation of Rotating Instabilities in a Low Speed Research Compressor," Third European Conference on Turbomachinery – Fluid Dynamcs and Thermodynamics, March 2-5, London, UK.

Mailach, R., Lehmann, I., and Vogeler, K., 2000, "Rotating Instabilities in an Axial Compressor Originating from the Fluctuating Blade Tip Vortex," ASME Paper 2001-GT-0299.

Mailach, R., Sauer, H., and Vogeler, K., 2001, "The Periodical Interaction of the Tip Clearance Flow in the Blade Rows of Axial Compressors," ASME Paper 2001-GT-0299.

Marz, J., Gui, X., and Neise, W., 1999, "On the Structure of Rotating Instabilities in Axial Flow Machines," ISABE 99-7252, Proceedings of the 14th International Symposium on Airbreathing Engines, Sept. 1999, Florence, Italy.

Marz, J., Hah, C., and Neise, W., 2001, "An Experimental and Numerical Investigation into the Mechanisms of Rotating Instabilty," ASME Paper 2001-GT-0536.

Vo, H. D., 2001, "Role of Tip Clearance Flow on Axial Compressor Stability," Massachusetts Institute of Technology, September 2001.